JOURNAL OF MATERIALS SCIENCE 8 (1973) 1296–1306

The stability of sapphire whiskers in nickel at elevated temperatures

Part 2 *The kinetics of morphological changes over the temperature range 1100 to 1400°C*

A. J. STAPLEY
Defence Standards Laboratories, Maribyrnong, Victoria, Australia
C. J. BEEVERS
Department of Physical Metallurgy and Science of Materials, University of Birmingham, UK

Composites of 1 to 20 vol % sapphire whiskers contained in a nickel matrix were annealed in vacuum in the temperature range 1100 to 1400° C for times up to 1000 h. After annealing, whiskers and alumina particles were extracted from composites and examined by optical and electron microscopy. The change of the aspect ratio distribution of whiskers during annealing was determined and related to the theory of tip ovulation. Pronounced spheroidization of whiskers occurred. This was only partly due to ovulation from the tips of whiskers by interfacial diffusion. Ostwald ripening made a significant contribution to the extent of spheroidization. For sapphire whiskers in nickel, ovulation times and interfacial diffusion constants were determined. The activation energy for the growth of ovoidal particles increased from 35 to 110 kcal during spheroidization. This is believed to indicate that the rate controlling process changes from interfacial diffusion to bulk matrix diffusion as the rate of tip ovulation decreases during annealing.

1. Introduction

Some of the microstructures formed and chemical changes undergone by sapphire whiskers on annealing in nickel have been described previously [1, 2]. Some quantitative measurements of the extent of spheroidization are now reported and discussed.

The processes which may be responsible for decreasing the aspect ratio of whiskers during annealing will now be described.

1.1. Ostwald ripening

The growth of the larger particles at the expense of the smaller ones in order to minimize the interfacial free energy is termed Ostwald ripening. Dromsky *et al* [3] found that for alumina particles in nickel the mean interparticle separation increases with the cube root of time. This was interpreted by Oriani [4] (contrary to the conclusion of the authors) as indicating that the rate-controlling step during Ostwald ripening in this system is volume diffusion in the matrix. The significance of Ostwald ripening for alumina whiskers in nickel may be great since the diffusional distances in the nickel matrix are of the same order (10 μm) as in Dromsky *et al's* composites. On the other hand the driving force for the process is the energy difference between small and large particles, and the present sapphire whiskers are bounded by low energy planes, e.g., {0001}, $\{10\bar{1}1\}$, $\{11\bar{2}0\}$. Also the whiskers are mostly large (1 to 3 μm diameter) compared with the initial size (*ca.* 50 nm) of the alumina particles that are observed to coarsen. The surface area to volume ratio, and hence, the interfacial energy per unit volume is less for these whiskers than for Dromsky *et al's* particles. A decisive factor could be the difference in interfacial energy per unit volume between a whisker and an equiaxed particle of the same diameter. Some approximate values of interfacial energy for sapphire whiskers in nickel were presented in Part 1 [2].

1.2. Ovulation

Tip-ovulation was predicted by Nicholls and

Mullins [5] from an analysis of the effect of surface diffusion and both internal and external volume diffusion on the change in shape of bodies of various original geometry. These authors consider that interface diffusion should predominate where, as in the present case, the diffusion distances are < 50 μm. In this case, assuming a hemispherical tip on a whisker with a cylindrical shank, ovulation is predicted to occur in the following sequence: the tip of the whisker blunts and forms a bulbous shape on the end of the whisker with a neck of decreasing radius behind it. The radius of this neck decreases with time until finally it reaches zero causing an egg-shaped particle to separate from the whisker. This process will be repeated as long as ample length of whisker remains. Micrographs demonstrating ovulation are shown in Part 1 and a quantitative analysis of the process using formulae given by Nicholls and Mullins is presented below.

1.3. Waisting

Waisting is another process predicted by Nicholls and Mullins [6]. In this case instability occurs at longitudinal perturbations with wavelengths greater than the cylindrical circumference of the whisker under consideration. Growth steps and side branches on whiskers are suitable sites for this to occur. This process is demonstrated in Fig. 12 of [1].

1.4. Constant volume shape changes

Shape changes at constant volume are also to be expected if surface diffusion is extensive compared with volume diffusion. In this process material is transferred from the ends of a whisker along the surface to the middle, causing the shape to approach a sphere thus minimizing the surface area per unit volume.

1.5. Critical aspect ratio for sapphire whiskers in nickel

Estimates of the critical aspect ratio of sapphire whiskers for the reinforcement of nickel depend [7] on whether the ultimate shear strength of the matrix (T') is greater or less than that of the matrix/whisker interface (S). The critical aspect ratio is given by:

$$\frac{l_c}{d} = \frac{\sigma_f}{2T} \quad (1)$$

assuming whiskers of round cross-section of diameter d where l_c = critical whisker length, σ_f = ultimate tensile strength of whisker, and the value substituted for T is the lesser of the two quantities, S and T'. Recent work by Nicholas [8] indicates that at 20°C S is less than T' and the critical aspect ratio could then be as high as 53. Interface shear strengths at elevated temperatures are not as yet available. On the other hand, Kelly's assumption [7] that the shear strength is approximately half of the ultimate tensile strength leads to critical aspect ratios of e.g., 11 at 20°C, 59 at 1000°C and 178 at 1200°C. The average aspect ratio of sapphire whiskers as grown is 500 to 5000; they can, therefore, be used to reinforce nickel at room and elevated temperatures provided that fragmentation during incorporation into the matrix is not excessive and that further reductions of aspect ratio due to diffusional shape changes at elevated temperatures are small. It has been demonstrated that pronounced diffusional shape changes of sapphire whiskers in nickel may occur at elevated temperatures [1, 2]. The extent of these processes is presented herein as a statistical analysis giving results of more general applicability to this type of composite.

2. Experimental

Composites of sapphire whiskers in nickel were prepared and annealed for up to 1000 h at 1100 to 1400°C and the whiskers were then extracted for examination as described in [1] and [2]. The following considerations were taken into account in assessing the aspect ratios of the whiskers.

1. Surface tension effects caused the longer whiskers to be clustered into groups, thus obscuring their ends and making them difficult to measure. The stacking of whiskers in groups also caused foreshortening, reducing the apparent aspect ratio.

2. Focusing errors and diffraction fringes had a greater effect on the measured width than on the measured length of whiskers, decreasing the apparent aspect ratio.

3. "Barrel" distortion was occasionally noticed near the edges of electron micrographs taken at comparatively low magnifications. In these cases measurements were confined to the distortion-free centre of the micrographs.

4. A tendency to avoid photographing and measuring particular areas was reduced by taking neighbouring pictures along a linear traverse.

5. Equiaxed particles of reaction product (e.g. the spinel $NiAl_2O_4$), nonmetallic inclusions

(e.g. NiO) and spheroidized whiskers could not be distinguished due to the large number of measurements. Measurements were, therefore, confined to extracts that were shown by X-ray diffraction to be relatively free from reaction products and nonmetallic inclusions.

6. Random variations within each extract were minimized by the use of large samples of at least 160 whiskers. Checks on different micrographs from seven extracts gave variations of 6 to 14% in the percentage by numbers of ovules with aspect ratios between 1 and 3.

A factor (ld^2) proportional to the volume of each whisker was derived, where l = length and d = width measured as above. These whiskers mostly have a parallelogram cross-section with a width to thickness ratio of 2:1 to 5:1 [9] and are aligned with their width normal to the direction of viewing and measured as d on micrographs. The mean width to thickness ratio is not expected to vary unless altered by solution and growth effects during annealing. These effects would cause errors in the mean volume per whisker which is comparative rather than absolute. The normalized volume percentage of whiskers within each aspect ratio group for individual extracts are each subject to an identical error and should, therefore, be approximately correct.

From the measurements, histograms of aspect ratio versus both number percentage and volume percentage of whiskers were prepared for extracts after various annealing treatments. Owing to space restrictions these figures are not presented here, but are available elsewhere [10]. An l/d ratio of 3:1 has been arbitrarily chosen as representing the dividing line between ovules and whiskers, so that the histograms may be summarized into the information presented below.

3. Results

The percentage number of whiskers having $1 < l/d < 3$ increased with annealing time at 1100, 1200, 1300 and 1400° C as shown in Fig. 1. Lines in this figure are drawn for the 20 vol % hot-pressed composite ZCE. The results of measurements on other composites are identified by the final letter indicating each composite below, plus a sample number. The types of composite are as follows:

Type of composite	*Identity mark*
Hot-pressed 1 vol % whiskers	ZCT
Hot-pressed 20 vol % whiskers	ZCD,ZCE,ZCG
Cold-pressed and sintered (5 vol % whiskers)	ZCZ
Settled and roll-bonded (core 5 vol % whiskers)	ZCP

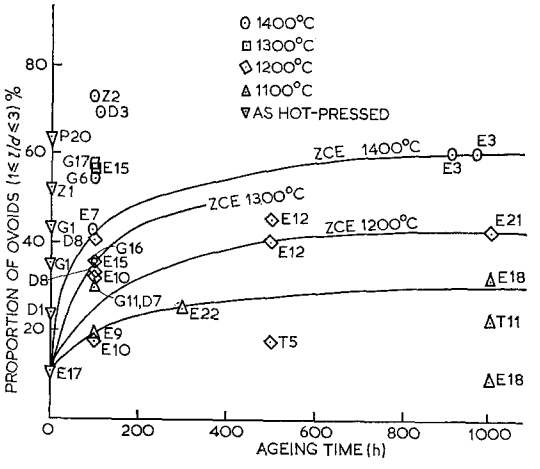

Figure 1 Number percentage of whiskers having $1 < l/d < 3$ as a function of annealing time at 1100 to 1400° C.

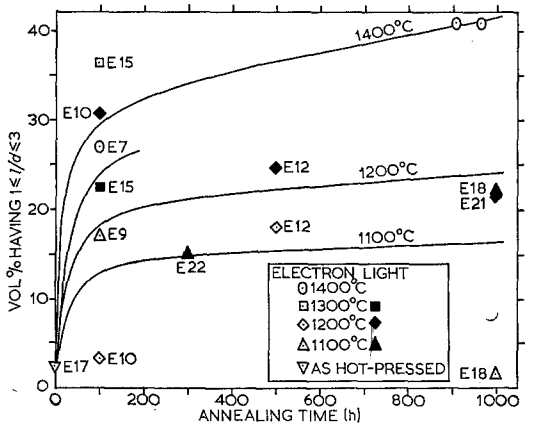

Figure 2 The variation of the volume percentage of whiskers having $1 < l/d < 3$ with annealing time at 1100 to 1400° C in the 20 vol % composite ZCE.

The data below are for the composite ZCE only. For this composite the volume percentage of whiskers having $1 < l/d < 3$ increases with time at temperature (Fig. 2) in a similar way to the proportion by numbers. Measurements from electron micrographs showed important differences from measurements made on light micrographs. The number of whiskers detected

in light micrographs decreases as the width decreases below 1 μm. This contrasts with electron micrographs which show increasing numbers of whiskers as the width decreases to 0.2 μm. The aspect ratio distributions both by numbers and by volume also show pronounced differences between data derived from electron and light micrographs.

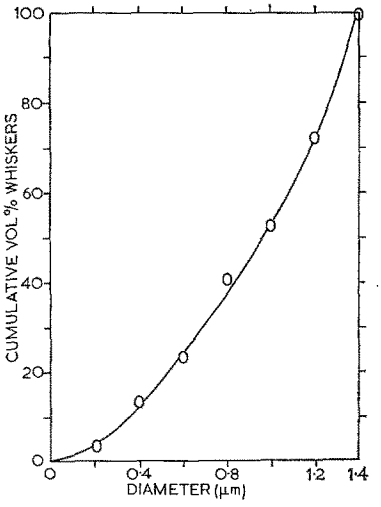

Figure 3 Cumulative volume percentage of whiskers in the hot to pressed composite ZCE versus their diameter.

TABLE I Numbers and volume of the finest particles and whiskers

Treatment	No. % < 0.4 μm diameter	Vol % < 0.4 μm diameter
As hot-pressed	74.7	13.0
1000 h/1100°C	66.3	8.4
100 h/1200°C	62.3	9.9
500 h/1200°C	50.4	3.7
100 h/1300°C	40.1	3.7
100 h/1400°C	40.8	3.2
912 to 967 h/1400°C	5.5	0.06

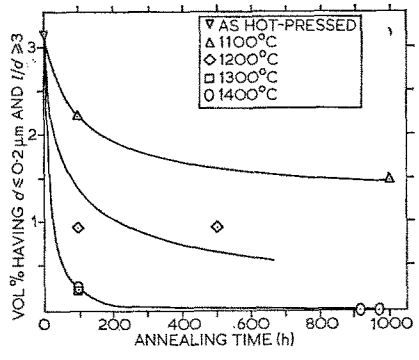

Figure 4 The volume percentage of those whiskers from the composite ZCE having $d < 0.2$ μm and $l/d >$ as a function of time at temperature.

The cumulative volume percentage of whiskers as a function of their diameter in the composite ZCE as hot-pressed is plotted in Fig. 3. The maximum whisker diameters observed in each extract from light micrographs are higher than those measured on electron micrographs. There is considerable scatter in the maximum diameters observed but they appear to increase with both time and temperature of annealing. In contrast with the supplier's quoted diameter range of 1 to 3 μm, electron micrographs show the presence of increasing numbers of whiskers as the diameter decreases below 1 μm in tape as-fired and in a 20 vol % composite (ZCE) as hot-pressed. However, the proportion by volume of whiskers decreases with decreasing width.

From numbers and volume diameter histograms the following amounts of both whiskers and ovules finer than 0.4 μm diameter were found.

Fig. 4 shows the volume percentage of those whiskers having both $d < 0.2$ μm and $l/d > 3$ as a function of annealing time. Only data from electron micrographs is included in Fig. 4 because of the 0.1 μm limit of resolution in optical microscopy.

The logarithm of the number percentage of whiskers having $1 < l/d < 3$ is plotted against the logarithm of the annealing time in Fig. 5. The slope of the resulting straight lines varies from 0.21 to 0.39 indicating that the number of ovules is proportional to approximately the cube root of the annealing time. A similar plot of the logarithm of the volume percentage of ovules versus the logarithm of annealing time (Fig. 6) has straight lines with gradients of 0.15 to 0.17; this indicates that the volume ovulated is proportional to approximately the sixth root of the annealing time.

The logarithm of the annealing time is plotted against the reciprocal of the absolute temperature for constant volume proportions of ovules in Fig. 7. It is assumed that the several concurrent physical processes, namely ovulation, waisting, Ostwald ripening, constant volume spheroidization which are responsible for spheroidization each occur at a rate that is limited by the slowest of several consecutive

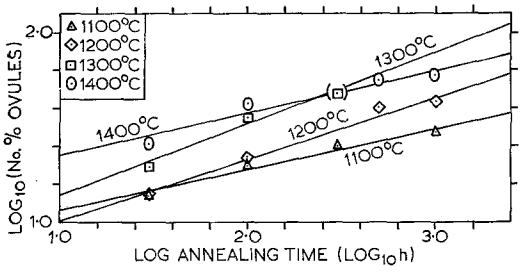

Figure 5 The logarithm of the number percentage of ovules (i.e. those whiskers having $1 < l/d < 3$) as a function of the logarithm of annealing time in the 20 vol % composite ZCE.

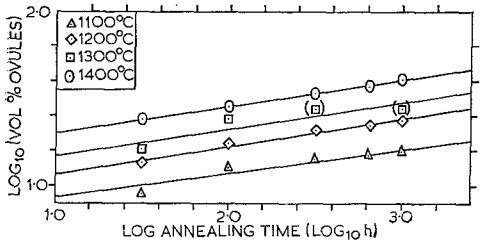

Figure 6 The logarithm of the volume percentage of ovules versus the logarithm of annealing time in the 20 vol % composite ZCE.

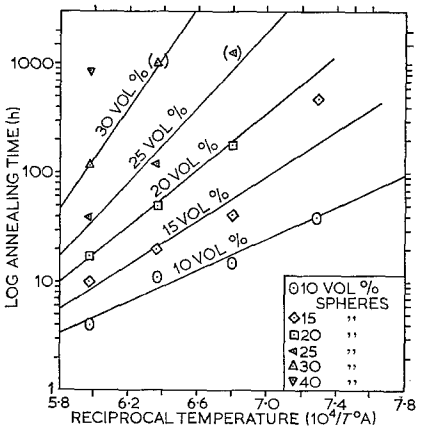

Figure 7 The variation with the reciprocal of the absolute temperature of the logarithm of the annealing time producing a constant volume proportion of ovules.

steps, and these steps may be similar for each process. An Arrhenious equation is applied in order to define what the slowest step might be:

$$A_T = A_0 e^{-Q/RT} \quad (2)$$

where A_T = annealing time (h) producing a given volume proportion of spheres, A_0 and Q are constants, R = gas constant, T = absolute temperature. A_0 and Q are derived from the intercepts and gradients respectively in Fig. 7 using the logarithm of Equation 2, giving the results shown in Table II. The activation energy

TABLE II Pre-exponential (A_0) constants and activation energies (Q) at intervals during spheroidization

Vol % ovules	A_0 (h)	Q (kcal mol^{-1})
10	1.1×10^{-4}	35.2
15	3.5×10^{-6}	48.6
20	5.5×10^{-7}	57.3
25	3.2×10^{-9}	77.1
30	5.9×10^{-13}	109.9

Q of the rate controlling process increases as the proportion of ovules increases.

The mean volume per whisker was found to increase with the time and temperature of annealing as shown in Fig. 8.

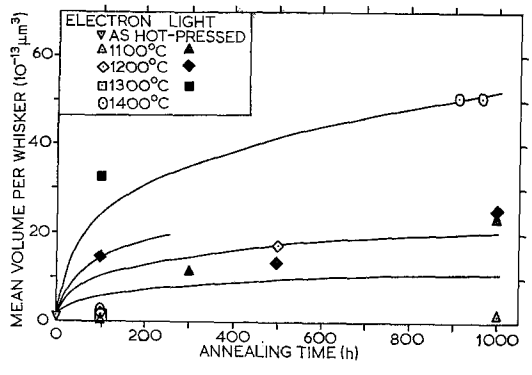

Figure 8 The mean volume per whisker as a function of the annealing time at various temperatures in the 20 vol % composite ZCE.

4. Discussion

For practical applications the life to rupture of alumina whiskers/nickel composites under known stresses at 1100 to 1200° C needs to be determined. The present results may enable qualitative estimates of these data to be made. Improvements [11] in techniques of producing composites have now enabled high aspect ratios to be retained after hot-pressing. Although the present results were obtained using whiskers of relatively low aspect ratio they enable some

predictions to be made of the thermal stability of later potentially more useful composites.

Measurements on light micrographs yield different results from measurements from electron micrographs due to decreasing detection of whiskers in light micrographs as their width approaches the 0.1 μm optical limit of resolution. In the following discussion greater emphasis is therefore placed on the results derived from electron micrographs, although measurements made optically yield some useful information.

The decreasing rate of spheroidization with time is apparent from Figs. 1 and 2 and may result from the combined effects of the following three factors: (i) depletion of the more rapidly ovulating thinner whiskers (cf Fig. 4 and Table I); (ii) reduction of the number of whiskers available for spheroidization due to the shorter ones being consumed first; (iii) Ostwald ripening removing the finest ovules.

Nicholls and Mullins [6] predict that the thinner whiskers should ovulate more rapidly according to a fourth power law as follows:

$$t = \frac{4415}{B}\left(\frac{\pi r_o}{16}\right)^4 \qquad (3)$$

where $B = D_s\gamma\Omega^2\nu/KT$ (Equation 4), r_o = initial radius of whisker (assumed circular), D_s = surface diffusion coefficient, γ = surface tension (assumed isotropic), Ω = atomic volume, ν = number of diffusing surface atoms per unit surface area (conveniently $\nu = \Omega^{-2/3}$ [6]), K is Boltzmann's constant, and T is the temperature.

Theoretical ovulation times as a function of whisker radius are shown in Fig. 9; the times are dependent on the parameter B. The decreasing proportion of fine whiskers and particles as time and temperature are increased (Table I) is possibly due to concurrent spheroidization and Ostwald ripening. The maximum whisker width observed as hot-pressed, 1.4 μm, should upon tip ovulation result in ovules of 2.6 μm maximum diameter [6]. However, after 912 to 967 h at 1400°C, 70 vol %, i.e., 17 no. % of whiskers had a diameter greater than 2.6 μm. This may be a consequence of assumptions involved in the theory, but is more probably due to Ostwald ripening.

The longest whiskers present as hot-pressed had an aspect ratio between 44 and 55. Since a whisker recedes 3.35 times its initial radius during each ovulation period [6] complete spheroidization of these whiskers would require

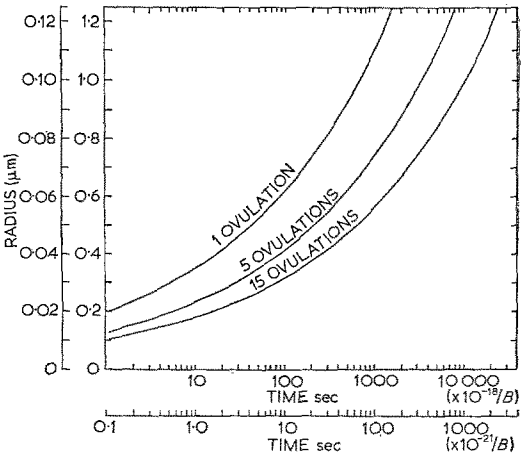

Figure 9 The variation with radius of the theoretical ovulation time from Equation 3.

13 to 16 ovulations from each end. However, the majority of the whiskers by volume as hot-pressed had $l/d < 15$ corresponding to only one to five ovulations for spheroidization to be essentially complete. Thus when some of the shorter whiskers have completely spheroidized the rate of further spheroidization would decrease in a manner dependent on the initial distribution of aspect ratios. This factor probably has less influence in decreasing the rate of spheroidization than the depletion of the thinnest whiskers. In order to distinguish a possible effect due to the depletion of the shortest ones, whiskers of constant diameter would be needed and this is only approximated by the present approach of grading the measurements into incremental groups in steps of 0.2 μm diameter. The ovulation period of whiskers having diameters of 0.2 μm or less is derived below and shows that tip ovulation is not the only process which could occur. In Fig. 9 curves are presented for one ovulation, for five ovulations (corresponding to spheroidization of the majority of the whiskers) and for fifteen ovulations (corresponding to complete spheroidization) based on the distribution of aspect ratios in as hot-pressed composites. Ostwald ripening decreases the number of small particles observed in Fig. 1 and is one of the reasons for making an assessment (Fig. 2) in terms of volume ratios. However, reprecipitation probably occurs more onto whiskers than onto equiaxed particles due to the greater surface area per unit volume of the whiskers, thereby

decreasing the observed ratio of spheres to whiskers. Thus an initial distribution of fine spheres may be replaced after longer annealing times by whiskers of greater diameter.

Furthermore, reprecipitation of alumina onto whiskers would increase their diameter and automatically decrease their rate of tip ovulation. In Fig. 8, the 100 h data points derived from electron micrographs are low because of rapid spheroidization of fine whiskers, an effect which is not detected in optical microscopy due to the lack of fine resolution. This low mean volume per whisker indicates that for short times ($\sim$ 100 h) of annealing the rate of ovulation of fine particles exceeds their rate of solution into the matrix. The subsequent increase in mean whisker volume indicates that after longer times of annealing ($\sim$ 500 h at 1200°C) any fine particles ovulated must be rapidly taken into solution and reprecipitated onto whiskers or particles of greater volume.

The above qualitative explanation for the decreasing rate of spheroidization may be summarized as follows: Whiskers of low diameter spheroidize rapidly, the shorter ones disappear first, and the resulting fine particles go preferentially into solution in the matrix.

4.1. The rates of tip ovulation

The volume proportion of the finest whiskers ($d < 0.2$ μm) remaining unspheroidized is shown in Fig. 4 as a function of annealing time. Ovulation times and B values are derived as follows:

From Fig. 4 the volume fraction of unspheroidized whiskers having $d < 0.2$ μm decreases from 3.14 vol % as hot-pressed to 0.002 vol % after 200 h at 1400°C. Virtually all these whiskers from the very smallest diameters up to and including 0.2 μm diameter would be spheroidized by this treatment. Only the longest whiskers originally present as hot-pressed would remain in (shortened) whisker form, i.e., the longest 0.002 vol % fraction found to have $l/d > 50$ as hot-pressed [10]. Since the number, N, of ovulations for complete destruction of a whisker of length l accounting for both ends is $l/3.35d$ [6], all the whiskers having $l/d < 50$ would have ovulated up to $50/3.35 = 14.9$ times. The time, t, per ovulation would, therefore, have been 200 h/14.9 = 13.4 h or less for the thinner whiskers. Now, the fourth power law indicates an ovulation period for 0.1 μm radius whiskers (Fig. 9) of $6.56 \times 10^{-20}/B$ sec. Equating the latter theoretical ovulation time with that derived above gives:

$$B_{1400} = \frac{6.56 \times 10^{-20}}{13.4 \times 3600} = 1.4 \times 10^{-24} .$$

In the same way, values of B at 1200 and 1100°C can be estimated. However, for these two temperatures, spheroidization of the finest whiskers ($d < 0.2$ μm) was incomplete (Fig. 4) after the longest annealing times studied. It is probable that those whiskers remaining unspheroidized within the 0 to 0.2 μm diameter range were those of greatest diameter d *ca.* 0.2 μm rather than those of greatest original length prior to annealing. A plot of cumulative vol % whiskers having diameters up to and including the maximum of each 0.2 μm increment in ZCE17 as hot-pressed (Fig. 3) allows estimation of the diameter d_{ov} below which whiskers are completely ovulated. The data derived are as follows:

Temperature	1100°C	1200°C
time	1000 h	217 h
fraction ovulated (Fig. 4)	1.6 vol %	2.1 vol %
original l/d ratio now completely ovulated	55	55
N	55/3.35=16.4	55/3.35=16.4
t	1000/16.4=60.9 h	217/16.4=13.2 h
d_{ov} (Fig. 3)	0.12 μm	0.16 μm
t (from fourth power law, Fig. 9)	$8.7\times10^{-21}/B$sec	$27.1\times10^{-21}/B$ sec
B	4.0×10^{-26}	5.7×10^{-25}

Substituting for B in the fourth power law enables the ovulation period for whiskers of various diameters at 1100, 1200 and 1400°C to be calculated. The rates of ovulation (Table III) are insufficient to account for the observed increases in the volume proportion of spheres with annealing time. As an example the volume proportion of spheres resulting from tip ovulation is approximately estimated below for an anneal of 100 h at 1400°C and compared with observed data on sample ZCE 7. The fractional volume reduction of a whisker per ovulation $\triangle V$, allowing for both ends is approximately:

$$\triangle V = \frac{ld^2 - (l - 3.35d)d^2}{ld^2} = \frac{3.35d}{l} .$$

The number of ovulations, N, in 100 h at 1400°C can be derived from Table III for whiskers within each 0.2 μm diameter increment. The volume

TABLE III Predicted ovulation periods (h) at 1100 to 1400°C

Whisker radius (μm)	1100°C	1200°C	1400°C
0.03	3.69	0.26	0.11
0.05	27.71	2.00	0.86
0.1	463.0	32.02	13.39
0.2	7 360	512.5	214.1
0.3	37 210	2 592	1 083
0.4	120 500	8 390	3 510
0.5	277 100	20 010	8 560
0.6	603 000	42 000	17 750
0.7	1 098 000	76 900	32 180
1.0	4 630 000	320 200	133 900
1.2	9 540 000	664 000	277 900

proportion of spheres V_{ov} resulting from ovulation of whiskers within each 0.2 μm diameter increment is obtained from the relation

$$V_{ov} = VN \triangle V = \frac{VN\,3.35d}{l}$$

where V is the original as hot-pressed volume proportion of whiskers having $l/d > 3$ in a given diameter increment. The fractional volume reduction $\triangle V$ depends on the original aspect ratio as hot-pressed, which is observed to decrease with increasing diameter [10]. (Many more measurements would be required to indicate whether random sampling errors alone are responsible for this decrease.) Predictions for the volume proportion of ovulated particles after 100 h at 1400°C assuming that all the whiskers within each diameter increment had the same original l/d ratio of 15, 20 or 55 are compared with the observed proportion in Table IV. It is apparent that the theory of tip ovulation can account for only approximately half of the observed proportion of ovules; also most of the predicted ovules are formed from whiskers having diameters less than 0.6 μm, whereas most of those observed have diameters greater than

TABLE IV Observed proportion of particles having $1 \leqslant l/d \leqslant 3$ and predicted proportion of ovulated particles for an anneal of 100 h at 1400°C

Whisker diameter (μm)	V* (vol %)	N†	Predicted proportion ovulated V_{ov} vol % assuming an original aspect ratio of:			Observed vol % spheres in ZCE 7
			$l/d = 15$	$l/d = 20$	$l/d = 55$	
0–0.2	3.1	> 1000 –7.5	3.1	3.1	3.1 –1.3	0.01
0.21–0.4	9.2	7.5 –0.47	9.2 –0.96	9.2 –0.72	3.9 –0.26	0.44
0.41–0.6	10.0	0.47 –0.09	1.04–0.21	0.78–0.16	0.28–0.06	1.82
0.61–0.8	17.2	0.092–0.029	0.36–0.11	0.27–0.08	0.10–0.03	4.31
0.81–1.0	11.3	0.03 –0.01	0.07–0.03	0.05–0.02	0.02–0.008	2.07
1.01–1.2	18.3	0.01 –0.006	0.05–0.02	0.04–0.02	0.01–0.006	2.42
1.21–1.4	28.0	0.006–0.003	0.04–0.002	0.03–0.001	0.01–0.0005	0
1.41–1.6	0		0	0	0	1.97
1.61–1.8	0		0	0	0	4.64
1.81–2.0	0		0	0	0	4.51
2.01–2.2	0		0	0	0	4.69
0–2.2	97.1		13.91–4.47	13.52–4.14	5.71–1.70	26.88

*V = original volume of whiskers having $l/d > 3$.
†N = no. of ovulations in 100 h.

0.6 μm. Ostwald ripening accounts for this by preferentially removing the finest ovules and reprecipitating them onto both whiskers and spheres of larger diameter. The prediction of any ovulation during an anneal of 100 h at 1400°C for whiskers having diameters greater than 0.4 μm is unjustified since $N < 1$. At temperatures of 1100 and 1200°C values of N are lower still and the tip ovulation theory again only partly accounts for the observed extent of spheroidization. The discrepancy between these predictions and the experimental observations can be ascribed to the operation of the other processes.

It is also possible to estimate interfacial diffusivities by substituting in Equation 4 using values of B derived above. Rearranging Equation 4, the surface diffusivity, D_S, is given by

$$D_S = \frac{KTB}{\gamma\Omega^{4/3}} \quad (5)$$

with symbols as defined previously. According to Feingold and Li [12], D_S should be an effective diffusion coefficient influenced by a composition constraint as well as by the individual diffusivities of each of the three species of atom (Ni, Al and O) that are being transported. Since interfacial diffusivities in this system are unknown a coupled diffusion analysis [12] cannot be applied and D_S has been estimated by substituting in turn the atomic volumes (Ω) of nickel, aluminium and oxygen in Equation 4. These estimated interfacial diffusivities are compared with surface and volume diffusivities from the literature in Table V. The estimated values show a striking but possibly fortuitous similarity to the volume self-diffusivities of nickel; nickel is also the slowest of the three atom species for bulk diffusion in nickel. Table V also verifies the experimental fact that alumina whiskers annealed in the absence of the nickel matrix for 100 h at 1400°C show no detectable spheroidization [2]; volume diffusivities in alumina are approximately six orders of magnitude lower than those in nickel and surface diffusivities in alumina, by comparison between volume and surface self-diffusion in nickel, may possibly be two orders of magnitude less than those in nickel.

4.2. The kinetics of the spheroidization process

The results have shown that the rate of spheroidization of sapphire whiskers in nickel during annealing depends upon the individual rates of three processes, namely: (i) tip-ovulation, (ii) waisting, (iii) Ostwald-ripening. A fourth process may also possibly affect numerous whiskers having original l/d values slightly greater than 3:1. This is: (iv) constant-volume shape changes.

These four processes are considered below on the basis that the following sequence of events probably occurs during annealing: (a) initially tip-ovulation of the finest whiskers predominates; these fine whiskers are thus reduced in numbers until (b) at longer annealing times one or more of the other three processes predominates, the rate of tip-ovulation having decreased.

The relative contributions to the observed proportion of ovules probably varies with temperature; the contributions of tip-ovulation and waisting vary with some function of annealing time; those of tip-ovulation and Ostwald ripening vary with some function of the whisker diameter; Ostwald ripening should produce an increase in mean volume per whisker proportional to $(\text{time})^{1/3}$ [3], shown as continuous curves in

TABLE V A comparison of estimated interfacial diffusivities with published data

	1100°C ($cm^2\ sec^{-1}$)	1200°C ($cm^2\ sec^{-1}$)	1400°C ($cm^2\ sec^{-1}$)
Estimated $D_{S,Ni}$	3.0×10^{-11}	4.8×10^{-10}	1.4×10^{-9}
Estimated $D_{S,Al}$	2.0×10^{-11}	3.3×10^{-10}	1.0×10^{-9}
Estimated $D_{S,O^{-2}}$	2.6×10^{-11}	4.1×10^{-10}	1.2×10^{-9}
D_S (Ni on Ni) [5], [13]	0.9×10^{-6}	1.5×10^{-6}	2.3×10^{-5}
D_V (Ni in Ni) [14]	3.06×10^{-11}	1.61×10^{-10}	2.45×10^{-9}
D_V (Al in Ni) [14]	1.26×10^{-10}	6.16×10^{-10}	8.38×10^{-9}
D_V (O in Ni) [15]	1.3×10^{-7}	1.6×10^{-6}	1.9×10^{-5}*
D_V (Fe in Al_2O_3 [16]	4.7×10^{-12}	9.2×10^{-12}*	2.8×10^{-11}*
D_V (Al in Al_2O_3) [17]	2.1×10^{-17}*	3.6×10^{-16}*	3.8×10^{-14}*
D_V (O^{2-} in Al_2O_3) [18]	4.40×10^{-17}	1.84×10^{-16}	$1.93 \times ^{-15}$

*extrapolated values.

Fig. 8 that correlate with the data points. The contribution of constant volume shape changes to the observed proportion of ovules will vary with aspect ratio. Whereas tip ovulation preferentially removes the thinner whiskers, waisting may affect whiskers of all diameters.

The formation of equiaxed aluminate particles by a reaction between nickel, alumina and traces of oxygen is discounted as the spinel $NiAl_2O_4$ was not detected by X-ray diffraction in the extracts under consideration, i.e., the amount present was < 5 vol %. Spinel formation is discussed in Part 1 [2].

Those whiskers having $3 < l/d < 6$ could possibly undergo constant-volume shape changes and enter the size range $l/d < 3$ arbitrarily classified as ovules. The composite ZCE17 as hot-pressed contains 34.9 vol % of whiskers having $3.1 < l/d < 6.0$, which could account for the observed quantities of ovules after annealing. However, the extent of this process may be small. In order for the volume of a whisker to be conserved upon spheroidization either the interfacial diffusivity or the diffusivity within the sapphire must be large compared with the diffusivity in the surrounding matrix. According to Table V this is not so; compared with bulk diffusion in nickel interfacial diffusion is of a similar magnitude and volume diffusion within sapphire is 6 orders of magnitude slower.

The initial proportion of whiskers having a low aspect ratio in the present composites (i.e. 92 vol % with $l/d < 20$) is high compared with that likely to be achieved in future (> 50 vol % with $l/d > 200$ [11]). The contribution of tip-ovulation and constant volume shape changes in the present samples is therefore probably higher in the early stages and lower (owing to a decrease in numbers) in the later stages of annealing compared with future composites. This means that the rate constants of spheroidization from the present samples must be treated as only an approximate guide to spheroidization rates in other composites.

Each process may occur in several consecutive steps namely: (i) presumably alumina dissociates, (ii) the atoms or ions diffuse mainly along the interface except in Ostwald ripening where diffusion must be through the nickel matrix, and finally, (iii) the atoms or ions are reprecipitated. There is little difference in the steps involved for ovulation, waisting and constant volume shape changes. Ostwald ripening requires similar dissociation and reprecipitation stages. The rate of the overall change is the rate of the slowest individual step, and presumably the activation energy of the overall change characterizes this step. This indicates that diffusion is the rate controlling process since if one of the other steps were rate controlling the activation energy would remain constant. Oriani [4] and Feingold and Li [12] have accounted for the deviation of the effective activation energy for diffusion from the activation energies for diffusion of e.g. oxygen (74.4 kcal [15]) or aluminium (64.0 kcal [14]) in nickel. This variation in activation energy emphasizes that spheroidization is not the result of a single unique process. The increased activation energy at the higher degrees of spheroidization probably reflects a variation in the contribution from each of the four processes and may indicate a change from predominantly interface to predominantly bulk matrix diffusion.

For Ostwald ripening of alumina particles in nickel an activation energy of 84.7 ± 2.0 kcal and $(\text{time})^{1/3}$ dependence have been observed [3]. Fig. 6 indicates that the vol % of spheres is proportional to the sixth root of time. The spheroidization rate thus decreases more rapidly than the rate of Ostwald ripening. In Fig. 6, Ostwald ripening is contributing towards the increase in the vol % of ovules with time. By dissolving away the smaller particles, Ostwald ripening subtracts from a plot of the logarithm of numbers of ovules versus logarithm of annealing time (Fig. 5).

5. Conclusions

1. Alumina whiskers show a distinct lack of stability when used at elevated temperatures for fibre reinforcement in a nickel matrix.
2. The following processes can cause spheroidization during annealing of alumina whiskers dispersed in nickel: tip-ovulation, waisting, Ostwald ripening.
3. A tip-ovulation mechanism can account for approximately half of the observed volume fraction of spheres formed from sapphire whiskers annealed at 1400°C in nickel.
4. The values of the parameter B and of the interfacial diffusivity, D_s, that fit the theory of tip ovulation are as follows:

annealing temperature	1100°C	1200°C	1400°C
B	4.0×10^{-26}	5.7×10^{-25}	1.4×10^{-24}
$D_{s,Ni}$ (cm^2 sec^{-1})	3.0×10^{-11}	4.8×10^{-10}	1.4×10^{-9}

5. Contrary to observation in sapphire whisker/

nickel composites, the tip ovulation theory predicts that whiskers of diameter > 0.4 μm will only spheroidize after 7300 h at 1100°C, after 500 h at 1200°C or after 200 h at 1400°C.
6. During annealing of sapphire whiskers in nickel the volume fraction of ovoidal alumina particles increases as the sixth root of the annealing time. The numbers of these particles increase proportionally to the cube root of the annealing time.
7. On the basis that an Arrhenius equation describes spheroidization by several distinct processes of sapphire whiskers in nickel during annealing, the complex activation energy of the process increases from 35 to 110 kcal as the volume proportion of spheres increases from 10 to 30 vol% this variation in activation energy may reflect a change in the rate controlling process from interfacial diffusion to volume diffusion in the matrix.

Acknowledgements

The authors are indebted to Professor G. V. Raynor, FRS for provision of laboratory facilities and to AWRE, Aldermaston for financial support. The authors also wish to acknowledge the co-operation of Dr A. Moore and Dr C. Calow of AWRE, Aldermaston, in providing materials for this work.

References

1. A. J. STAPLEY and C. J. BEEVERS, *J. Mater. Sci.* **4** (1969) 65.
2. *Idem, ibid* **8** (1973) 1287.
3. J. A. DROMSKY, F. V. LENEL, and G. S. ANSELL, *Trans. Met. Soc. AIME* **224** (1962) 236.
4. R. A. ORIANI, *Acta Metallurgica* **12** 1964) 1399.
5. F. A. NICHOLLS and W. W. MULLINS, *Trans. Met. Soc. AIME* **233** (1965) 1840.
6. *Idem, J. Appl. Phys.* **36** (1965) 1826.
7. A. KELLY and G. J. DAVIES, *Met. Rev.* **10** (1965) 94.
8. M. NICHOLAS, *J. Mater. Sci.* **3** (1968) 571.
9. A. P. LEVITT, *Materials Research and Standards* **6** (1966) 64.
10. A. J. STAPLEY, Ph.D. thesis, University of Birmingham (1969).
11. C. A. CALOW, Atomic Weapons Research Establishment, Aldermaston, private communication (1968).
12. A. H. FEINGOLD and CHE-YU LI, *Acta Metallurgica* **16** (1968) 1101.
13. J. M. BLAKELY and H. MYKURA, *ibid* **9** (1961) 23.
14. C. J. SMITHELLS, "Metals Reference Book", 4th Ed. Vol. 2 (Butterworths, London, 1967).
15. R. BARLOW and P. J. GRUNDY, *J. Mater. Sci.* **4** (1969) 797.
16. V. IZVEKOV and K. GORBUNOVA quoted by B. I. BOLTAKS, "Diffusion in Semiconductors" (Infosearch Ltd, London 1963) p. 273.
17. A. E. PALADINO and W. D. KINGERY, *J. Chem. Phys.* **37** (1962) 957.
18. Y. OISHI and W. D. KINGERY, *ibid*, **33** (1960) 480.

Received 29 January and accepted 13 February 1973.